Image-guided cancer surgery using near-infrared fluorescence

Alexander L. Vahrmeijer[1,*], **Merlijn Hutteman**[1], **Joost R. van der Vorst**[1], **C.J.H. van de Velde**[1], and **John V. Frangioni**[3,4,*]

[1]Department of Surgery, Leiden, University Medical Center, Albinusdreef 2, 2333 ZA, Leiden, The Netherlands [3]Department of Medicine, Beth Israel Deaconess Medical Center, 330 Brookline Avenue, Boston, MA 02215 [4]Department of Radiology, Beth Israel Deaconess Medical Center, 330 Brookline Avenue, Boston, MA 02215

Abstract

Paradigm shifts in surgery arise when surgeons are empowered to perform surgery faster, better, and/or less expensively. Optical imaging that exploits invisible near-infrared fluorescent light has the potential to improve cancer surgery outcomes while minimizing anesthesia time and lowering healthcare costs. Because of this, the last few years have witnessed an explosion of proof-of-concept clinical trials in the field. In this review, we introduce the concept of near-infrared fluorescence imaging for cancer surgery, review the clinical trial literature to date, outline the key issues pertaining to imaging system and contrast agent optimization, discuss limitations and leverage, and provide a framework for making the technology available for the routine care of cancer patients in the near future.

Keywords

Near-infrared fluorescence imaging; clinical translation; intraoperative imaging; image-guided surgery; sentinel lymph node mapping; tumor margins

Introduction

Improvements in preoperative imaging techniques have made a meaningful impact on cancer patient care. However, during actual cancer surgery, the eyes and hands of the surgeon remain the dominant "imaging modalities" used to decide which tissue needs to be resected, i.e., malignant cells, and which tissue needs to be avoided, i.e., normal cells. Palpation and visual inspection are not always sufficient for discriminating between tissue types, though, leading to irradical resections or unnecessary removal of healthy tissue. In breast cancer, for example, many of which are non-palpable, margin positivity rates range from 5 to 49%.[1,2] In some cases, ultrasound and/or x-ray fluoroscopic imaging are used

during cancer surgery, but these modalities lack the possibility of using targeted contrast agents to specifically visualize certain cell types, expose patient and caregiver to ionizing radiation, and/or require direct contact with the body. Intraoperative MRI and CT scanning have played a significant role as well, especially in the field of neurosurgical image guidance.[3] However, intraoperative systems are costly and complex, and are currently used mainly for neurosurgery at major medical centers.

Over the past several years, intraoperative imaging using invisible near-infrared (NIR) fluorescent light has entered the surgical theatre to fill the gap between preoperative imaging and intraoperative reality.[4,5] Whereas visible light penetrates tissue on a micron scale, NIR light (700 nm – 900 nm) can travel millimeters, up to centimeters, through tissue.[6] Because tissue exhibits almost no autofluorescence in the NIR spectrum, the signal-to-background can be maximized using NIR fluorescent contrast agents, creating "white stars in a black sky".[7] In addition, it does not use ionizing radiation, making it an inherently safe technique provided that attention is paid to laser illumination levels. And, as NIR light is invisible to the human eye, it does not alter the look of the surgical field, thus minimizing the learning curve.

Specialized intraoperative imaging systems for open surgery,[8–14] laparoscopy,[15,16] thoracoscopy,[17,18] and robotic surgery[19,20] have recently become available for clinical trials.[21] Using these systems, NIR fluorescent contrast agents can be visualized with acquisition times in the millisecond range, enabling real-time guidance during surgery (Figure 1).

To date, NIR fluorescent contrast agents specific for many different targets have been developed, including agents for cancer cells,[22–24] sentinel lymph nodes,[25–27], neurological diseases, [28,29] cardiovascular diseases,[30,31] skeletal processes,[32] renally cleared agents for ureter imaging,[33] and hepatically cleared agents for bile duct imaging.[34] Optically-active nerve cell agents[35,36] have also been described, but are yet to achieve NIR wavelengths.

Although these research results lay the foundation for a future revolution in patient care, excitement in the field needs to be tempered with the reality of the underlying physics. Like visible light, NIR light is attenuated by absorption and scatter in living tissue. In fact, total attenuation (the sum of attenuation due to absorption and scatter) is exponential as a function of depth. Thus, only 1-millionth to 1-billionth of the photons launched into a tissue as fluorescence excitation is even potentially recoverable as fluorescence emission, and only 10–25% of these photons are truly recoverable because of the finite quantum yield of most NIR fluorophores. Taken together, depth of detection for even bright targets will be constrained to ≈ 5 mm, but could be slightly more or less depending on the particular tissue's optical properties. While this is more than adequate for tumor margin detection and many surgical applications, it requires leveraging of the technology with other imaging modalities in some clinical situations (discussed below).

Absorption and scatter also limit the ability to quantify NIR fluorescent signals. Without knowing (or measuring) absorption, scatter, and anisotropy of the tissue being imaged, only qualitative information can be inferred (reviewed in [37]). Correction for attenuation of excitation light[38] can certainly assist with target detection, although over-compensation can also cause false-positives. Full correction for optical properties can provide quantitative measurements of NIR fluorescent signal.[39,40] However, the use of quantitative metrics for intraoperative decision-making is still in its infancy. In the case of cancer margin detection, a qualitative present/absent is the relevant metric, and for perfusion studies, relative signal over time after injection of a tracer provides quantitative information without requiring the measurement of tissue optical properties.[41,42]

This review focuses on the clinical applications of NIR fluorescence imaging in cancer surgery, recent developments, and the long-term potential benefit for patients.

Clinical applications of NIR fluorescence imaging

Intraoperative NIR fluorescence imaging depends on the availability of a NIR fluorescent contrast agent and an intraoperative imaging system to visualize the otherwise invisible contrast agent during surgery.[4] Indocyanine green (ICG) is the only 800 nm NIR fluorescent contrast agent that is approved for this clinical indication by the Food and Drug Administration (FDA) and the European Medicines Agency (EMEA). Methylene blue (MB) has been applied clinically for many years as a visible (dark blue) contrast agent. As MB was introduced into clinical practice in an era when no formal approval was needed, no evaluation by the FDA, EMEA, or comparable authorities has been performed, but it remains widely used. When sufficiently diluted, MB acts as a 700 nm fluorophore and has recently been used in NIR fluorescence clinical studies.[43–45].

5-aminolevulinic acid (5-ALA) is the major substrate for protoporphyrin synthesis and has been used clinically for tumor detection (fluorescence imaging) and tumor treatment (photodynamic therapy). 5-ALA (typically administered in a topical or oral form) induces synthesis and accumulation of the fluorescent molecule protoporphyrin IX (PpIX) in epithelia and neoplastic tissues, among them malignant gliomas and meningiomas.[46–48] PpIX has two major fluorescence emission peaks with approximately half of its fluorescence emission centered $\approx$ 700 nm (i.e., NIR). 5-ALA has been studied extensively in the field of neurosurgery as described below.

Interestingly, because MB, 5-ALA-induced PpIX, and ICG have distinct spectral properties, they could theoretically be used simultaneously in the same patient, provided that the imaging system is capable of discriminating one from the other. Neither ICG, MB, nor 5-ALA are ligand-targeted contrast agents. The first clinical report of non-targeted (non-NIR) fluorescence surgical imaging dates back to 1948, when Moore et al used fluorescein in neurosurgical interventions for the localization of brain tumors.[49] The first clinical report of targeted (non-NIR) fluorescence surgical imaging dates back to 1992, when Folli and colleagues used carcinoembryonic antigen-targeted antibodies labeled with fluorescein to visualize colorectal carcinomas *in vivo* in patients.[50] In 2012, Van Dam and colleagues described the successful use of folate conjugated to fluorescein for intraoperative visualization of ovarian cancer cells for debulking surgery.[51] While these landmark studies provided essential proof-of-principle, fluorescein and other visible fluorophores are not optimal for cancer surgery because high absorption and scatter result in interrogation of only the surface layer, and, importantly, high autofluorescence from surrounding tissue reduces contrast.

Nevertheless, using the existing major NIR fluorophores, ICG, MB, and 5-ALA-induced PpIX, proof of principle clinical studies in several types of surgery have been performed in recent years (Table 1).

Sentinel lymph node mapping

Sentinel lymph node (SLN) mapping is standard-of-care in a variety of cancers, including breast cancer and cutaneous melanoma. Currently, most centers perform SLN mapping using a radioactive tracer, a visible blue dye such as isosulfan blue or patent blue, or a combination of the two. Although in most cases acceptable results are obtained using these methods, they both have some drawbacks. Visible blue dyes stain the patient and the surgical field and cannot be visualized below the surface of tissue. Radioactive tracers expose patients and caregivers to ionizing radiation, are expensive, and imaging suffers from

poor spatial and temporal resolution. For SLN mapping using NIR fluorescence imaging, contrast agents are injected at a low concentration with no staining of the surgical field, no ionizing radiation is used, and an improvement is observed over blue dyes in terms of depth sensitivity. For SLN mapping, targeted contrast agents are not necessary, and because ICG is clinically available, many SLN studies were undertaken as soon as the first intraoperative imaging systems became available (Figure 2; Table 1).[5] To date, NIR fluorescence-guided SLN mapping has been extensively studied in breast cancer,[11,52–56] as well as in colorectal cancer, [15,57–61] skin cancer,[62,63] cervical cancer,[13,64,65] vulvar cancer, [66–68] head and neck, [63,69,70] lung cancer, [17,71] penile cancer, [69] endometrial cancer,[72] gastric cancer, [73,74] and esophageal cancer. [75]

These first studies demonstrate the feasibility of NIR fluorescence imaging during surgery. Comparison of NIR fluorescence imaging to blue dyes indicates that NIR fluorescence imaging may substitute blue dyes, as it outperforms the blue dyes due to increased tissue penetration depth and lack of staining of the patient and the surgical field.[53,76,77] In particular in countries were radiotracers are not allowed or available, NIR fluorescence imaging could replace blue dyes as routine SLN mapping methodology. However, as current imaging systems in combination with ICG show depth penetration less than 1 centimeter, ongoing studies are assessing the non-inferiority of NIR fluorescence compared to radioactivity, which is of particular clinical significance when lymph nodes are located deeper within the patient, for example in more obese patients.

Combination of radioactivity and NIR fluorescence—To overcome the issue of limited depth penetration, a combination of NIR fluorescence and radioactivity has been reported for SLN mapping.[16,27,69,78] This combination is complementary: the superior depth penetration of radioactivity is used to perform gross navigation to the SLN, after which the superior spatial and temporal resolution of NIR fluorescence facilitates image-guided identification and resection of the SLN. When a preoperatively injected, combined NIR fluorescent and radioactive tracer is used, no intraoperative injection of tracer is necessary and the preoperative injection by the nuclear medicine physician suffices for both preoperative lymphoscintigraphy and intraoperative SLN detection, reducing the duration of surgery and anesthesia and potentially reducing costs.[16,27,69,78]

Targeted SLN tracers—An optimal tracer for SLN mapping migrates quickly from the injection site to the lymph node and remains in the first draining node without migrating to higher tier nodes. To prevent migration to higher tier nodes, radiotracers are commonly conjugated to a colloid to increase the hydrodynamic diameter or to a ligand to increase retention. In the United States, a sulfur-based colloid is most widely used, whereas in Europe, an albumin-based colloid is commonly used. Indocyanine green cannot be conjugated covalently to sulfur colloid without altering its chemical structure, although non-covalent adsorption of ICG to albumin and albumin nanocolloid appears to work well. [25,79] A novel strategy for lymph node retention has been developed by Vera and colleagues by creating a lymphatic tracer that is specific for a receptor (mannose-binding protein) found on reticuloendothelial cells of lymph nodes.[80] While this tracer was primarily designed for radiolabeling, recent studies have been published in which this tracer is conjugated to a fluorescent label. [26,81]

Tumor imaging

Although ICG's use in SLN mapping has paved the way for NIR fluorescence imaging in the operating room, one of the key applications in cancer surgery is intraoperative tumor visualization. In order to visualize tumors using NIR fluorescence imaging, a contrast agent should accumulate in or around a tumor. Although a variety of tumor specific NIR

fluorescent contrast agents have been developed and applied preclinically, none of these has obtained full clinical approval by either the FDA or the EMEA. Using the clinically available contrast agents ICG, MB, and 5-ALA first-in-human intraoperative tumor imaging studies have been described in various cancer types.

ICG—After intravenous administration, ICG is cleared by the liver, potentially enabling intraoperative identification of liver lesions. Indeed, Ishizawa and colleagues were the first to demonstrate clear visualization of both colorectal liver metastases and hepatocellular carcinomas (HCC).[82] In their study and subsequent studies, several hours to days after intravenous injection of ICG, a fluorescent rim could be visualized intraoperatively around the tumors, with almost no background signal in the surrounding healthy liver parenchyma.[83–85] Tumors that could be visualized using NIR fluorescence imaging were all relatively superficial (less than 8 mm below the liver surface), tumors located deeper could not be visualized by NIR fluorescence imaging.

Several clinical studies reported on NIR fluorescence imaging in patients suffering from HCCs using ICG.[10,82] Surprisingly, ICG accumulated in the HCCs itself, as opposed to the accumulation in a rim around colorectal liver metastases. Intraoperative ultrasound is routinely used before resection of liver tumors in order to identify tumors that were missed preoperatively. It is also used intraoperatively in conjunction with inspection and palpation. One of the main limitations of intraoperative ultrasound is the hampered detection of superficial and small tumors.[86] NIR fluorescence performs well in superficial and small tumors, but is unable to visualize deeper tumors. Therefore, in liver surgery, NIR fluorescence imaging can be seen as a potential adjunct to conventional imaging techniques for the preoperative and intraoperative detection of primary liver tumors and hepatic metastases. Satou and colleagues used NIR fluorescence imaging after ICG injection to identify extrahepatic metastases of HCC.[87] They report the detection of 5 metastases that were otherwise not detected in 2 out of 17 patients (11.7%), confirming the complementary value of NIR fluorescence imaging. Yokoyama and colleagues demonstrated that NIR fluorescence imaging after ICG injection identified hepatic metastases of pancreatic carcinoma that were otherwise not detected in 8 out of 49 patients (16.3%), potentially preventing those patients from unnecessary radical resections and associated morbidity.[88] A recent study by our group[89] found that in 5 of 40 patients (12.5%), ICG-based NIR fluorescence imaging detected colorectal metastases in liver that were otherwise undetectable by preoperative CT, intraoperative ultrasound, palpation, and visualization. As might be expected, all detectable metastases were less than 8 mm from the liver surface.

A novel and rapidly growing field of NIR fluorescence guided cancer surgery is related to neurosurgery. ICG has been used to intraoperatively identify high-grade gliomas, meningiomas, hemangioblastomas and pituitary tumors.[90–92] The previously mentioned tumors could be visualized by intravenously administering 5 to 25 mg ICG.

After intravenous injection, ICG binds to plasma proteins, thereby increasing its hydrodynamic diameter. This potentially enables ICG to accumulate in tumors due to enhanced permeability and retention. In 2006, Horowitz and colleagues presented the use of ICG via this mechanism for intraoperative detection of ovarian cancer metastases.[93]

MB—MB has previously been described to stain parathyroid glands and insulinomas the color blue after high-dose intravenous and intra-arterial injection, respectively.[94,95] Winer and colleagues demonstrated preclinically that dilute MB can be used as an NIR fluorescent contrast agent for identifying insulinomas.[43] Although clinical use of MB for insulinomas has not yet been reported, it was successfully used to visualize a rare solitary fibrous tumor of the pancreas in a patient.[45]

5-ALA—5-ALA-induced PpIX has been studied extensively in the field of neurosurgery, mostly to intraoperatively identify brain tumors such as malignant gliomas. Stummer et al. showed that visualization of PpIX fluorescence after 5-ALA administration (oral administration) led to a significant increase in the incidence of complete resection (65% compared to 36%), improved progression-free survival at 6 months (41% compared to 21%), fewer reinterventions, and delayed onset of neurological deterioration.[48,96] Furthermore, 5-ALA-induced PpIX has been used to identify the hardly visible urothelial bladder cancer during fluorescence guided cystoscopies which was reviewed by Jocham et al.[97]

Topical contrast agents—Besides systemically injected contrast agents, topical application of NIR fluorescence contrast agents can be of benefit, for example in colonoscopic or cystoscopic procedures. The successful use of 5-ALA and derivatives has been described in bladder cancer.[98–100] Although visible (red) light fluorescence was used for imaging in these studies, the tumor cell-synthesized Protoporphyrin IX actually has half its emission spectrum in the NIR.

Imaging of vital structures

Iatrogenic damage to vital structures occurs frequently during cancer surgery. For example, nerve damage is relatively common and can result in postoperative pain or loss of specific functions, such as incontinence or impotence, especially in rectal cancer or prostate cancer surgery. Damage to ureters or bile ducts is relatively rare, but both are associated with severe complications, such as renal dysfunction and biliary peritonitis. Damage to these structures is usually a result of inadequate identification during surgery. For this purpose, NIR fluorescence imaging has also been described for intraoperative identification of vital structures. As ICG is cleared by the liver and excreted into the bile ducts, studies have described intraoperative NIR fluorescence cholangiographies after intravenous administration of ICG.[20,101] Using MB, which is cleared predominantly by the kidneys, ureters could be identified intraoperatively using NIR fluorescence imaging (Figure 2).[44] Due to their pelvic location, ureters can be difficult to visualize, in particular when tumor or inflamed tissue is covering them. The increased depth penetration of NIR fluorescence can therefore be of added value over visible light imaging. NIR fluorescence imaging can be of particular benefit in laparoscopic and robotic surgery, where there is diminished tactile feedback. NIR fluorescence-capable fiberscopic systems are now readily available for these applications. Finally, subcutaneously administered ICG has been used in multiple clinical studies to visualize lymphatic flow in real-time, which will likely aid in understanding the mechanism of lymphedema, a morbid complication of several cancer surgeries.[55,102]

Vascularization

Vascular perfusion of anastomoses—Anastomotic leaks after intestinal surgery for cancer remain a relatively common and severe complication.[103] Occurrence of anastomotic leaks is presumably caused by insufficient perfusion of an intestinal anastomosis. NIR fluorescence can be used to visualize blood perfusion after intravenous injection of ICG. Several groups reported on its ability to assess anastomotic blood perfusion after intestinal surgery.[104–106] Although retrospectively studied, Kudszus and colleagues described a reduction in the risk of revision due to anastomotic leak by 60% in patients whose anastomosis was examined using NIR fluorescence angiography compared to historically matched patients without imaging.[104]

Vascular perfusion of flaps in reconstructive surgery—Vessel identification and selection is essential during cancer reconstructive surgery using free or pedicled flaps. NIR fluorescence imaging provides the opportunity to identify vessels intraoperatively and to

assess perfusion in these flaps.[107,108] In breast reconstructive surgery, NIR fluorescence angiography has been used for vessel identification and selection, and to monitor venous outflow.[109,110] Newman and colleagues describe in their study that arterial and venous problems were identified intraoperatively in 4 out of 8 (50%) patients, which changed the operative plan in 3 of 4 cases, leading to a 100% flap survival outcome.[109]

Key parameters: target, contrast agent dose, and timing

Optimal visualization is achieved by maximizing the signal-to-background ratio, thus maximizing contrast. In order to do so, the chosen target, the type of contrast agent, the route of administration (i.e. intravenous, local injection, topical spray), and the imaging goal (i.e. sentinel lymph node mapping, tumor imaging, etc.) all have to be factored in.

Perhaps the most important parameter for imaging is the target. Is it an abundant receptor on the cell surface, a sub-cellular organelle, or the substrate for a membrane transporter? Because all fluorescent techniques rely on concentration, the abundance and availability of the target are key concerns. Keep in mind, for example, that a cell surface receptor with a total number of receptors per cell (BMax) of 10^4 can only achieve a fluorophore concentration of ≈ 17 nM, assuming a 1:1 ratio of targeted NIR fluorophore to receptor. Even the most highly abundant receptors, with a BMax of 10^5–10^6 can only achieve $\approx 1~\mu M$ concentration.

Within the first few seconds after intravenous injection, NIR fluorescent contrast agents highlight the arterial then venous systems (Figure 3). Over the next minutes to hours, hepatic and/or renal clearance will occur in parallel with tissue biodistribution and target binding. Some NIR fluorophores, such as MB, accumulate in certain cells by unknown mechanisms. Others are either targeted to particular receptors or membrane transporters, or accumulate passively due to structural abnormalities in the tissue (e.g., the enhanced permeability and retention or EPR effect).[111]

As the contrast agent clears from the bloodstream and normal tissues, and hopefully retained in tumor tissue, the SBR at the target site increases. In order to determine the necessary dose and timing, dosing, biodistribution, and pharmacokinetic studies are therefore essential. For example, an imaging time too short relative to clearance will result in a low SBR due to high background. Conversely, an imaging time too long relative to target binding will result in a low SBR due to loss of signal.

In SLN mapping, the contrast agent migrates from the injection site to the sentinel lymph node. Depending on the contrast agent's characteristics, flow to higher tier nodes might occur over time. To prevent misidentification of the SLN, dynamic imaging can be employed, starting directly after injection. Although counterintuitive, injection of a concentration of fluorophore that is too high results in a decrease of SLN signal due to quenching.[4] In dose-finding studies for SLN mapping, an ICG injection concentration of 500 μM in a volume of 1.6 mL was found to be optimal, although these numbers may vary among tumor types, and the distance between injection site and the SLN.[12]

Current developments

Clinical studies have demonstrated the feasibility of intraoperative imaging using near-infrared fluorescence in various applications. These studies, however, are based on contrast agents that were already available clinically. In order to determine the true clinical benefit of this technique, development and clinical assessment of contrast agents tailored to specific applications is essential.

Contrast agent development and optimization

Development of novel NIR fluorescent contrast agents is dependent on the availability of clinically-compatible fluorophores. Although many fluorophores have been evaluated in a preclinical setting, to date only two fluorophores have been reported to be in the process of clinical translation: IRDye 800CW (LI-COR Biosciences, Lincoln, NE) and ZW800-1 (The FLARE Foundation, Wayland, MA). Both compounds are small molecules, characterized as non-toxic in initial toxicity studies and are conjugatable to targeting moieties. In addition to their ability to be conjugated to various targeting ligands, the purely renal clearance of ZW800-1, and the combined renal and hepatic clearance of IRDye 800CW, enable these agents to be used for imaging of ureters and bile ducts.

As recently reviewed by Scheuer and colleagues,[112] clinically approved targeted antibodies are available for various tumors and tumor markers, for example bevacizumab (Genentech, San Francisco, CA) against the vascular endothelial growth factor A, cetuximab against the epidermal growth factor receptor (Bristol-Myers Squibb, New York City, NY, and Eli Lilly, Indianapolis, IN), and trastuzumab against the human epidermal growth factor receptor 2 (Genentech, San Francisco, CA). Combining these already approved antibodies with a NIR fluorophore could usher in a new generation of NIR fluorescent contrast agents. Indeed, the first clinical trial using bevacizumab conjugated to IRDye 800CW has been approved and is accruing patients.[113] In addition to antibodies, other targeting molecules, such as peptides, have been successfully translated into the clinical using radiolabeling and suggest potential for NIR fluorescence imaging. For example integrin αVβ3 targeting using cyclic arginine-glycine-aspartic acid (cRGD) has been demonstrated clinically in positron emission tomography studies.[114] A fluorophore conjugated to this peptide has been described preclinically for tumor imaging (cRGD-ZW800-1).[23] To overcome disadvantages of intact antibodies, investigational contrast agents are being developed using smaller antigen binding fragments such as nanobodies.[115] Nanobodies have a smaller hydrodynamic diameter and can therefore extravasate more easily than intact antibodies, even in areas of high interstitial pressure (i.e., solid tumors). Indeed, nanobodies against the epidermal growth factor receptor have been shown to outperform whole antibodies for tumor imaging.[116] As heterogeneity in tumors is an important problem when selecting a targeting ligand,[117] it is likely that a cocktail of several targeted NIR fluorophores will be employed once more tumor-specific ligands are developed and tested.

In order to visualize nerves, several research groups are developing specific contrast agents. One approach is focused on a family of fluorescent dyes that bind to the myelin of nerves.[118] However, these contrast agents currently fluoresce in the non-optimal visible spectrum. Another approach is the use of NIR fluorescent peptides that bind to nerve sheaths.[35] No clinical trial has yet been reported on nerve-specific agents, although the field eagerly awaits such a development.

A distinct class of NIR fluorescent contrast agents encompasses activatable agents. These agents are non-fluorescent or low-fluorescent in the unactivated state, and become fluorescent after activation by a molecular target, such as a tumor-specific enzyme. Preclinical studies show adequate tumor detection after intravenous injection of activatable agents. [22,24,119–121] Other reports show rapid tumor visualization after topical application of activatable agents.[122] Several of these agents are in the process of obtaining regulatory approval for proof-of-principle trials, however, to date no such trials are approved and accruing patients.

Imaging system development and optimization

Over the last few years, various imaging systems have been developed for intraoperative NIR fluorescence imaging by academic and industry groups.[8–11,13–20,120] Besides imaging systems for open surgery, NIR fluorescence imaging systems are available for laparoscopic, thoracoscopic, and robotic surgery. Most of these systems mark the first production grade development iteration, with optimized successors being developed.

Key issues that inform imaging system design are the fluorescence excitation light, the optics, usability (ergonomics), and cost. Maximizing the fluence rate of the excitation light increases tissue penetration depth. However, for laser-based light sources, skin/eye exposure, irreversible photochemical bleaching of the NIR fluorophore, and tissue heating are the limiting factors. In general, fluence rates are limited to the $10–25$ mW/cm^2 range in order to avoid these issues and the need for laser goggles. Initial imaging system prototypes were often assembled using off-the-shelf optics, which can distort and attenuate NIR light, causing suboptimal detection of NIR fluorescence.[4] Current versions of NIR fluorescence imaging systems are manufactured with optimized optics for NIR light and do not suffer from these problems. The possibility of visualizing multiple contrast agents simultaneously, for example for tumor identification and nerve visualization, would be beneficial. For this purpose, imaging systems are in development that can simultaneously acquire multiple wavelengths. [11,13] Furthermore, techniques are being implemented to discriminate between contrast agents that emit at a similar wavelength. [123,124] Finally, ergonomics, both physical and the use of software and advanced algorithms to improve the efficiency of clinical workflow, should be a focus of attention during imaging system design.

Limitations and leverage

Despite improved tissue penetration when compared to visible light, an essential limitation of NIR fluorescence imaging remains the inability to visualize structures more than approximately $5 – 8$ mm below the surface using current reflectance-based systems. Rather than introduce more complex optical methods, such as tomography, into surgery, the field has been migrating towards the combination of reflectance optical imaging with other modalities. Imaging modalities based on radioactive tracers, such as preoperative PET and SPECT, and intraoperative gamma probes and gamma cameras, have depth sensitivity to several cm but cannot provide real-time and precise visualization. Intraoperative ultrasound imaging also has superior depth penetration when compared to NIR fluorescence, but requires tissue contact and has problems visualizing smaller and superficial lesions. Combining NIR fluorescence imaging with these modalities leverages the key benefits, whilst overcoming the limited penetration depth of NIR light (Figure 4).[125] Another major limitation is the lack of clinically-available targeting agents. This is due to the high cost[126] and complex regulatory requirements surrounding drug development. Nevertheless, several academic and commercial groups have made progress on clinical translation and it is expected that several first-in-human clinical trials of new NIR fluorophores will commence within the next 2–3 years.

Path to routine patient care

NIR fluorescence imaging has been proven feasible during surgery in many clinical studies. The main question, however, is when will it become part of routine patient care? In the past, the adoption of a new technology had to satisfy only two major criteria. It needed to "change patient management," that is, make a meaningful impact on care, and it had to be "clinically realistic," that is, it couldn't disrupt normal workflow.[4] Nowadays, though, as insurance companies and governments try to reign in healthcare spending, technology must also make patient care faster, better, and cheaper. Optical imaging is one of the few technologies with

the potential to satisfy all three criteria. NIR fluorescence enables intraoperative imaging in real-time, without impeding the current clinical workflow. If surgeons are able to find tumors or avoid normal structures more easily then operating room time could be shortened. This in turn reduces anesthesia time and its associated risks, and means that surgeons can operate on more patients each day and hospitals can increase resource utilization. If improved tumor resection and/or normal tissue avoidance lowers recurrences and complication rates, then the healthcare system will enjoy huge cost savings. Quantification of these potential benefits, though, will require well-designed and well-executed clinical trials.

Conclusions

NIR fluorescence image-guidance during cancer surgery has the potential to improve patient management by visualizing tissue demarcation in real-time, thereby increasing the completeness of surgery and decreasing the morbidity associated with damage to normal structures. Intraoperative imaging requires a synchronous interplay between contrast agents, tumor biology, imaging systems, and algorithms. Results to date using available contrast agents and first generation imaging systems are extremely promising. Due to the relatively low depth penetration, NIR fluorescence imaging will likely be a complementary adjuvant to other imaging modalities, such as ultrasound and radioscintigraphy, in some clinical applications. Although studies focused on patient outcome and healthcare resource utilization should begin using existing imaging systems and non-targeted contrast agents, the era of targeted contrast agents for specific cancers remains on the precipice. Given the interest in the field, the next decade should clarify the role of NIR fluorescence imaging in cancer surgery and the extent to which it empowers surgeons to improve patient outcome.

Acknowledgments

References

1. Rizzo M, et al. The effects of additional tumor cavity sampling at the time of breast-conserving surgery on final margin status, volume of resection, and pathologist workload. Ann Surg Oncol. 2010; 17:228–234. [PubMed: 19636625]

2. McLaughlin SA. Surgical management of the breast: breast conservation therapy and mastectomy. Surg Clin North Am. 2013; 93:411–428. [PubMed: 23464693]

3. Kubben PL, et al. Intraoperative MRI-guided resection of glioblastoma multiforme: a systematic review. Lancet Oncol. 2011; 12:1062–1070. [PubMed: 21868286]

4. Gioux S, Choi HS, Frangioni JV. Image-guided surgery using invisible near-infrared light: fundamentals of clinical translation. Mol Imaging. 2010; 9:237–255. [PubMed: 20868625]

5. Schaafsma BE, et al. The clinical use of indocyanine green as a near-infrared fluorescent contrast agent for image-guided oncologic surgery. J Surg Oncol. 2011; 104:323–332. [PubMed: 21495033]

6. Chance B. Near-infrared images using continuous, phase-modulated, and pulsed light with quantitation of blood and blood oxygenation. Ann N Y Acad Sci. 1998; 838:29–45. [PubMed: 9511793]

7. Frangioni JV. In vivo near-infrared fluorescence imaging. Curr Opin Chem Biol. 2003; 7:626–634. [PubMed: 14580568]

8. Phillips BT, et al. Intraoperative Perfusion Techniques Can Accurately Predict Mastectomy Skin Flap Necrosis in Breast Reconstruction. Plast Reconstr Surg. 2012; 129:778e–788e.

9. Hirche C, et al. An Experimental Study to Evaluate the Fluobeam 800 Imaging System for Fluorescence-Guided Lymphatic Imaging and Sentinel Node Biopsy. Surg Innov. 201210.1177/1553350612468962

10. Gotoh K, et al. A novel image-guided surgery of hepatocellular carcinoma by indocyanine green fluorescence imaging navigation. J Surg Oncol. 2009; 100:75–79. [PubMed: 19301311]

11. Troyan SL, et al. The FLARE intraoperative near-infrared fluorescence imaging system: a first-in-human clinical trial in breast cancer sentinel lymph node mapping. Ann Surg Oncol. 2009; 16:2943–2952. [PubMed: 19582506]

12. Mieog JSD, et al. Toward optimization of imaging system and lymphatic tracer for near-infrared fluorescent sentinel lymph node mapping in breast cancer. Ann Surg Oncol. 2011; 18:2483–2491. [PubMed: 21360250]

13. Crane LMA, et al. Intraoperative multispectral fluorescence imaging for the detection of the sentinel lymph node in cervical cancer: a novel concept. Mol Imaging Biol. 2011; 13:1043–1049. [PubMed: 20835767]

14. Yamauchi K, Nagafuji H, Nakamura T, Sato T, Kohno N. Feasibility of ICG Fluorescence-Guided Sentinel Node Biopsy in animal Models using the HyperEye Medical System. Ann Surg Oncol. 201110.1245/s10434-010-1499-9

15. Cahill RA, et al. Near-infrared (NIR) laparoscopy for intraoperative lymphatic road-mapping and sentinel node identification during definitive surgical resection of early-stage colorectal neoplasia. Surg Endosc. 2011; 26:197–204. [PubMed: 21853392]

16. van der Poel HG, Buckle T, Brouwer OR, Valdés Olmos RA, van Leeuwen FWB. Intraoperative laparoscopic fluorescence guidance to the sentinel lymph node in prostate cancer patients: clinical proof of concept of an integrated functional imaging approach using a multimodal tracer. Eur Urol. 2011; 60:826–833. [PubMed: 21458154]

17. Moroga T, et al. Thoracoscopic segmentectomy with intraoperative evaluation of sentinel nodes for stage I non-small cell lung cancer. Ann Thorac Cardiovasc Surg. 2012; 18:89–94. [PubMed: 22082811]

18. Yamashita SI, et al. Video-assisted thoracoscopic indocyanine green fluorescence imaging system shows sentinel lymph nodes in non-small-cell lung cancer. J Thorac Cardiovasc Surg. 2011; 141:141–144. [PubMed: 20392454]

19. Borofsky MS, et al. Near-infrared fluorescence imaging to facilitate super-selective arterial clamping during zero-ischaemia robotic partial nephrectomy. BJU Int. 201210.1111/j.1464-410X. 2012.11490.x

20. Spinoglio G, et al. Real-time near-infrared (NIR) fluorescent cholangiography in single-site robotic cholecystectomy (SSRC): a single-institutional prospective study. Surg Endosc. 201210.1007/s00464-012-2733-2

21. Imaging system, contrast agents, and clinical trials in NIR fluorescence-guided surgery database. www.theflarefoundation.org at <http://www.theflarefoundation.org/knowledge-bank/>

22. Weissleder R, Tung CH, Mahmood U, Bogdanov A. In vivo imaging of tumors with protease-activated near-infrared fluorescent probes. Nat Biotechnol. 1999; 17:375–378. [PubMed: 10207887]

23. Choi HS, et al. Targeted zwitterionic near-infrared fluorophores for improved optical imaging. Nat Biotechnol. 2013; 31:148–153. [PubMed: 23292608]

24. Olson ES, et al. Activatable cell penetrating peptides linked to nanoparticles as dual probes for in vivo fluorescence and MR imaging of proteases. Proc Natl Acad Sci U S A. 2010; 107:4311–4316. [PubMed: 20160077]

25. Ohnishi S, et al. Organic alternatives to quantum dots for intraoperative near-infrared fluorescent sentinel lymph node mapping. Mol Imaging. 2005; 4:172–181. [PubMed: 16194449]

26. Emerson DK, et al. A receptor-targeted fluorescent radiopharmaceutical for multireporter sentinel lymph node imaging. Radiology. 2012; 265:186–193. [PubMed: 22753678]

27. Brouwer OR, et al. Feasibility of sentinel node biopsy in head and neck melanoma using a hybrid radioactive and fluorescent tracer. Ann Surg Oncol. 2012; 19:1988–1994. [PubMed: 22207047]

28. Hyde D, et al. Hybrid FMT-CT imaging of amyloid-beta plaques in a murine Alzheimer's disease model. Neuroimage. 2009; 44:1304–1311. [PubMed: 19041402]

29. Pham W, et al. Crossing the blood-brain barrier: a potential application of myristoylated polyarginine for in vivo neuroimaging. Neuroimage. 2005; 28:287–292. [PubMed: 16040255]

30. Deguchi JO, et al. Inflammation in atherosclerosis: visualizing matrix metalloproteinase action in macrophages in vivo. Circulation. 2006; 114:55–62. [PubMed: 16801460]

31. Sosnovik DE, et al. Fluorescence tomography and magnetic resonance imaging of myocardial macrophage infiltration in infarcted myocardium in vivo. Circulation. 2007; 115:1384–1391. [PubMed: 17339546]

32. Wunder A, Tung CH, Müller-Ladner U, Weissleder R, Mahmood U. In vivo imaging of protease activity in arthritis: a novel approach for monitoring treatment response. Arthritis Rheum. 2004; 50:2459–2465. [PubMed: 15334458]

33. Choi HS, et al. Synthesis and in vivo fate of zwitterionic near-infrared fluorophores. Angew Chem Int Ed Engl. 2011; 50:6258–6263. [PubMed: 21656624]

34. Figueiredo JL, Siegel C, Nahrendorf M, Weissleder R. Intraoperative near-infrared fluorescent cholangiography (NIRFC) in mouse models of bile duct injury. World J Surg. 2010; 34:336–343. [PubMed: 20033407]

35. Whitney MA, et al. Fluorescent peptides highlight peripheral nerves during surgery in mice. Nat Biotechnol. 2011; 29:352–356. [PubMed: 21297616]

36. Gibbs-Strauss SL, et al. Molecular imaging agents specific for the annulus fibrosus of the intervertebral disk. Mol Imaging. 2010; 9:128–140. [PubMed: 20487679]

37. Bradley RS, Thorniley MS. A review of attenuation correction techniques for tissue fluorescence. J R Soc Interface. 2006; 3:1–13. [PubMed: 16849213]

38. Themelis G, Yoo JS, Soh KS, Schulz R, Ntziachristos V. Real-time intraoperative fluorescence imaging system using light-absorption correction. J Biomed Opt. 2009; 14:064012. [PubMed: 20059250]

39. Valdés PA, et al. Quantitative, spectrally-resolved intraoperative fluorescence imaging. Sci Rep. 2012; 2:798. [PubMed: 23152935]

40. Saager RBR, Cuccia DJD, Saggese SS, Kelly KMK, Durkin AJA. Quantitative fluorescence imaging of protoporphyrin IX through determination of tissue optical properties in the spatial frequency domain. J Biomed Opt. 2011; 16:126013–126013. [PubMed: 22191930]

41. Matsui A, Lee BT, Winer JH, Laurence RG, Frangioni JV. Quantitative assessment of perfusion and vascular compromise in perforator flaps using a near-infrared fluorescence-guided imaging system. Plast Reconstr Surg. 2009; 124:451–460. [PubMed: 19644259]

42. Matsui A, Winer JH, Laurence RG, Frangioni JV. Predicting the survival of experimental ischaemic small bowel using intraoperative near-infrared fluorescence angiography. Br J Surg. 2011; 98:1725–1734. [PubMed: 21953541]

43. Winer JH, et al. Intraoperative localization of insulinoma and normal pancreas using invisible near-infrared fluorescent light. Ann Surg Oncol. 2010; 17:1094–1100. [PubMed: 20033320]

44. Verbeek FPR, et al. Intraoperative Near-Infrared Fluorescence-Guided Identification of the Ureters using Low-Dose Methylene Blue: A First-in-Human Experience. J Urol. 201310.1016/j.juro. 2013.02.3187

45. van der Vorst JR, et al. Near-infrared fluorescence imaging of a solitary fibrous tumor of the pancreas using methylene blue. World J Gastrointest Surg. 2012; 4:180–184. [PubMed: 22905287]

46. Colditz MJ, Jeffree RL. Aminolevulinic acid (ALA)-protoporphyrin IX fluorescence guided tumour resection. Part 1: Clinical, radiological and pathological studies. J Clin Neurosci. 2012; 19:1471–1474. [PubMed: 22959448]

47. Colditz MJ, Leyen KV, Jeffree RL. Aminolevulinic acid (ALA)-protoporphyrin IX fluorescence guided tumour resection. Part 2: theoretical, biochemical and practical aspects. J Clin Neurosci. 2012; 19:1611–1616. [PubMed: 23059058]

48. Stummer W, et al. Fluorescence-guided surgery with 5-aminolevulinic acid for resection of malignant glioma: a randomised controlled multicentre phase III trial. Lancet Oncol. 2006; 7:392–401. [PubMed: 16648043]

49. Moore GE, Peyton WT. The clinical use of fluorescein in neurosurgery; the localization of brain tumors. J Neurosurg. 1948; 5:392–398. [PubMed: 18872412]

50. Folli S, et al. Immunophotodiagnosis of colon carcinomas in patients injected with fluoresceinated chimeric antibodies against carcinoembryonic antigen. Proc Natl Acad Sci U S A. 1992; 89:7973–7977. [PubMed: 1518823]

51. van Dam GM, et al. Intraoperative tumor-specific fluorescence imaging in ovarian cancer by folate receptor-α targeting: first in-human results. Nat Med. 2011; 17:1315–1319. [PubMed: 21926976]

52. Murawa D, Hirche C, Dresel S, Hünerbein M. Sentinel lymph node biopsy in breast cancer guided by indocyanine green fluorescence. Br J Surg. 2009; 96:1289–1294. [PubMed: 19847873]

53. Hojo T, Nagao T, Kikuyama M, Akashi S, Kinoshita T. Evaluation of sentinel node biopsy by combined fluorescent and dye method and lymph flow for breast cancer. Breast. 2010; 19:210–213. [PubMed: 20153649]

54. Kitai T, Inomoto T, Miwa M, Shikayama T. Fluorescence navigation with indocyanine green for detecting sentinel lymph nodes in breast cancer. Breast Cancer. 2005; 12:211–215. [PubMed: 16110291]

55. Sevick-Muraca EM, et al. Imaging of lymph flow in breast cancer patients after microdose administration of a near-infrared fluorophore: feasibility study. Radiology. 2008; 246:734–741. [PubMed: 18223125]

56. Hirche C, Murawa D, Mohr Z, Kneif S, Hünerbein M. ICG fluorescence-guided sentinel node biopsy for axillary nodal staging in breast cancer. Breast Cancer Res Treat. 2010; 121:373–378. [PubMed: 20140704]

57. Hirche C, et al. Ultrastaging of colon cancer by sentinel node biopsy using fluorescence navigation with indocyanine green. Int J Colorectal Dis. 2012; 27:319–324. [PubMed: 21912878]

58. Ankersmit M, van der Pas MHGM, van Dam DA, Meijerink WJHJ. Near infrared fluorescence lymphatic laparoscopy of the colon and mesocolon. Colorectal dis. 2011; 13 (Suppl 7):70–73. [PubMed: 22098524]

59. Hutteman M, et al. Clinical translation of ex vivo sentinel lymph node mapping for colorectal cancer using invisible near-infrared fluorescence light. Ann Surg Oncol. 2011; 18:1006–1014. [PubMed: 21080086]

60. Schaafsma BE, et al. Ex vivo sentinel node mapping in colon cancer combining blue dye staining and fluorescence imaging. J Surg Res. 201310.1016/j.jss.2013.01.003

61. van der Pas MHGM, et al. Laparoscopic Sentinel Lymph Node Identification in Patients with Colon Carcinoma Using a Near-Infrared Dye: Description of a New Technique and Feasibility Study. J Laparoendosc Adv Surg Tech. 2013 130311062310000. 10.1089/lap.2012.0407

62. Fujiwara M, Mizukami T, Suzuki A, Fukamizu H. Sentinel lymph node detection in skin cancer patients using real-time fluorescence navigation with indocyanine green: preliminary experience. J Plast Reconstr Aesthet Surg. 2009; 62:e373–8. [PubMed: 18556255]

63. van der Vorst JR, et al. Dose optimization for near-infrared fluorescence sentinel lymph node mapping in patients with melanoma. Br J Dermatol. 2013; 168:93–98. [PubMed: 23078649]

64. van der Vorst JR, et al. Optimization of near-infrared fluorescent sentinel lymph node mapping in cervical cancer patients. Int J Gynecol Cancer. 2011; 21:1472–1478. [PubMed: 22027751]

65. Furukawa N, et al. The usefulness of photodynamic eye for sentinel lymph node identification in patients with cervical cancer. Tumori. 2010; 96:936–940. [PubMed: 21388055]

66. Crane LMA, et al. Intraoperative near-infrared fluorescence imaging for sentinel lymph node detection in vulvar cancer: first clinical results. Gynecol Oncol. 2011; 120:291–295. [PubMed: 21056907]

67. Hutteman M, et al. Optimization of near-infrared fluorescent sentinel lymph node mapping for vulvar cancer. Am J Obstet Gynecol. 2012; 206:89.e1–5. [PubMed: 21963099]

68. Schaafsma BE, et al. Randomized comparison of near-infrared fluorescence lymphatic tracers for sentinel lymph node mapping of cervical cancer. Gynecol Oncol. 2012; 127:126–130. [PubMed: 22796548]

69. Brouwer OR, et al. Comparing the hybrid fluorescent-radioactive tracer indocyanine green-99mTc-nanocolloid with 99mTc-nanocolloid for sentinel node identification: a validation study using lymphoscintigraphy and SPECT/CT. J Nucl Med. 2012; 53:1034–1040. [PubMed: 22645297]

70. Bredell MG. Sentinel lymph node mapping by indocyanin green fluorescence imaging in oropharyngeal cancer - preliminary experience. Head Neck Oncol. 2010; 2:31. [PubMed: 21034503]

71. Yamashita SI, et al. Sentinel node navigation surgery by thoracoscopic fluorescence imaging system and molecular examination in non-small cell lung cancer. Ann Surg Oncol. 2012; 19:728–733. [PubMed: 22101727]

72. Holloway RW, et al. Detection of sentinel lymph nodes in patients with endometrial cancer undergoing robotic-assisted staging: A comparison of colorimetric and fluorescence imaging. Gynecol Oncol. 2012; 126:25–29. [PubMed: 22507531]

73. Tajima Y, et al. Sentinel node mapping guided by indocyanine green fluorescence imaging during laparoscopic surgery in gastric cancer. Ann Surg Oncol. 2010; 17:1787–1793. [PubMed: 20162462]

74. Tajima Y, et al. Sentinel node mapping guided by indocyanine green fluorescence imaging in gastric cancer. Ann Surg. 2009; 249:58–62. [PubMed: 19106676]

75. Kubota K, et al. Application of the HyperEye Medical System for esophageal cancer surgery: a preliminary report. Surg Today. 2013; 43:215–220. [PubMed: 22782594]

76. van der Vorst JR, et al. Randomized comparison of near-infrared fluorescence imaging using indocyanine green and 99(m) technetium with or without patent blue for the sentinel lymph node procedure in breast cancer patients. Ann Surg Oncol. 2012; 19:4104–4111. [PubMed: 22752379]

77. Hutteman M, et al. Randomized, double-blind comparison of indocyanine green with or without albumin premixing for near-infrared fluorescence imaging of sentinel lymph nodes in breast cancer patients. Breast Cancer Res Treat. 2011; 127:163–170. [PubMed: 21360075]

78. van den Berg NSN, et al. Concomitant radio-and fluorescence-guided sentinel lymph node biopsy in squamous cell carcinoma of the oral cavity using ICG-(99m)Tc-nanocolloid. Eur J Nucl Med Mol Imaging. 2012; 39:1128–1136. [PubMed: 22526966]

79. Buckle T, et al. A self-assembled multimodal complex for combined pre-and intraoperative imaging of the sentinel lymph node. Nanotechnology. 2010; 21:355101. [PubMed: 20689167]

80. Vera DR, Wallace AM, Hoh CK, Mattrey RF. A synthetic macromolecule for sentinel node detection: (99m)Tc-DTPA-mannosyl-dextran. J Nucl Med. 2001; 42:951–959. [PubMed: 11390562]

81. Ting R, et al. Fast 18F Labeling of a Near-Infrared Fluorophore Enables Positron Emission Tomography and Optical Imaging of Sentinel Lymph Nodes. Bioconjug Chem. 2010; 21:1811–1819. [PubMed: 20873712]

82. Ishizawa T, et al. Real-time identification of liver cancers by using indocyanine green fluorescent imaging. Cancer. 2009; 115:2491–2504. [PubMed: 19326450]

83. Uchiyama KK, et al. Combined use of contrast-enhanced intraoperative ultrasonography and a fluorescence navigation system for identifying hepatic metastases. World J Surg. 2010; 34:2953–2959. [PubMed: 20734045]

84. Peloso A, et al. Combined use of intraoperative ultrasound and indocyanine green fluorescence imaging to detect liver metastases from colorectal cancer. HPB (Oxford). 2013:n/a–n/a.10.1111/hpb.12057

85. Ishizuka M, et al. Intraoperative observation using a fluorescence imaging instrument during hepatic resection for liver metastasis from colorectal cancer. Hepatogastroenterology. 2011; 59:90–92. [PubMed: 22260827]

86. Sahani DV, et al. Intraoperative US in patients undergoing surgery for liver neoplasms: comparison with MR imaging. Radiology. 2004; 232:810–814. [PubMed: 15273336]

87. Satou S, et al. Indocyanine green fluorescent imaging for detecting extrahepatic metastasis of hepatocellular carcinoma. J Gastroenterol. 201210.1007/s00535-012-0709-6

88. Yokoyama N, et al. Real-time detection of hepatic micrometastases from pancreatic cancer by intraoperative fluorescence imaging: preliminary results of a prospective study. Cancer. 2012; 118:2813–2819. [PubMed: 21990070]

89. van der Vorst JR, et al. Near-Infrared Fluorescence-Guided Resection of Colorectal Liver Metastases. Cancer. 2013:1–26. In press.

90. Hwang SW, Malek AM, Schapiro R, Wu JK. Intraoperative use of indocyanine green fluorescence videography for resection of a spinal cord hemangioblastoma. Neurosurgery. 2010; 67:ons300–3. discussion ons303. [PubMed: 20679920]

91. Ferroli P, et al. Application of intraoperative indocyanine green angiography for CNS tumors: results on the first 100 cases. Acta Neurochir Suppl. 2011; 109:251–257. [PubMed: 20960352]

92. Hojo M, et al. Usefulness of tumor blood flow imaging by intraoperative ICG videoangiography in hemangioblastoma surgery. World Neurosurg. 201310.1016/j.wneu.2013.02.009

93. Horowitz NS, et al. Laparoscopy in the Near Infrared With Icg Detects Microscopic Tumor in Women With Ovarian Cancer. Int J Gynecol Cancer. 2006; 16:616–623.

94. Keaveny TV, Fitzgerald PA, McMullin JP. Selective parathyroid and pancreatic staining. Br J Surg. 1969; 56:595–597. [PubMed: 4183792]

95. Keaveny TV, Tawes R, Belzer FO. A new method for intra-operative identification of insulinomas. Br J Surg. 1971; 58:233–234. [PubMed: 4100889]

96. Roberts DW, et al. Coregistered fluorescence-enhanced tumor resection of malignant glioma: relationships between δ-aminolevulinic acid-induced protoporphyrin IX fluorescence, magnetic resonance imaging enhancement, and neuropathological parameters. Clinical article. J Neurosurg. 2011; 114:595–603. [PubMed: 20380535]

97. Jocham D, Stepp H, Waidelich R. Photodynamic diagnosis in urology: state-of-the-art. Eur Urol. 2008; 53:1138–1148. [PubMed: 18096307]

98. Kriegmair M, et al. Detection of Early Bladder Cancer by 5-Aminolevulinic Acid Induced Porphyrin Fluorescence. J Urol. 1996; 155:105–110. [PubMed: 7490803]

99. Jichlinski P, et al. Clinical evaluation of a method for detecting superficial surgical transitional cell carcinoma of the bladder by light-induced fluorescence of protoporphyrin IX following the topical application of 5-aminolevulinic acid: preliminary results. Lasers Surg Med. 1997; 20:402–408. [PubMed: 9142679]

100. Jichlinski P, et al. Hexyl aminolevulinate fluorescence cystoscopy: new diagnostic tool for photodiagnosis of superficial bladder cancer--a multicenter study. J Urol. 2003; 170:226–229. [PubMed: 12796694]

101. Ishizawa T, et al. Fluorescent cholangiography illuminating the biliary tree during laparoscopic cholecystectomy. Br J Surg. 2010; 97:1369–1377. [PubMed: 20623766]

102. Rasmussen JC, et al. Human Lymphatic Architecture and Dynamic Transport Imaged Using Near-infrared Fluorescence. Transl Oncol. 2010; 3:362–372. [PubMed: 21151475]

103. Hyman NN, Manchester TLT, Osler TT, Burns BB, Cataldo PAP. Anastomotic leaks after intestinal anastomosis: it's later than you think. Ann Surg. 2007; 245:254–258. [PubMed: 17245179]

104. Kudszus S, Roesel C, Schachtrupp A, Höer JJ. Intraoperative laser fluorescence angiography in colorectal surgery: a noninvasive analysis to reduce the rate of anastomotic leakage. Langenbecks Arch Surg. 2010; 395:1025–1030. [PubMed: 20700603]

105. Pacheco PE, Hill SM, Henriques SM, Paulsen JK, Anderson RC. The novel use of intraoperative laser-induced fluorescence of indocyanine green tissue angiography for evaluation of the gastric conduit in esophageal reconstructive surgery. Am J Surg. 2013; 205:349–353. [PubMed: 23414958]

106. Jafari MD, et al. The use of indocyanine green fluorescence to assess anastomotic perfusion during robotic assisted laparoscopic rectal surgery. Surg Endosc. 201310.1007/s00464-013-2832-8

107. Holm C, Mayr M, Höfter E, Ninkovic M. Perfusion zones of the DIEP flap revisited: a clinical study. Plast Reconstr Surg. 2006; 117:37–43. [PubMed: 16404245]

108. Lee BT, et al. The FLARE intraoperative near-infrared fluorescence imaging system: a first-in-human clinical trial in perforator flap breast reconstruction. Plast Reconstr Surg. 2010; 126:1472–1481. [PubMed: 21042103]

109. Newman MI, Samson MC. The application of laser-assisted indocyanine green fluorescent dye angiography in microsurgical breast reconstruction. J Reconstr Microsurg. 2009; 25:21–26. [PubMed: 18925547]

110. Newman M, Samson M, Tamburrino J, Swartz K. Intraoperative Laser-Assisted Indocyanine Green Angiography for the Evaluation of Mastectomy Flaps in Immediate Breast Reconstruction. J Reconstr Microsurg. 2010; 26:487–492. [PubMed: 20539977]

111. Kosaka N, Mitsunaga M, Longmire MR, Choyke PL, Kobayashi H. Near infrared fluorescence-guided real-time endoscopic detection of peritoneal ovarian cancer nodules using intravenously injected indocyanine green. Int J Cancer. 2011; 129:1671–1677. [PubMed: 21469142]

112. Scheuer W, van Dam GM, Dobosz M, Schwaiger M, Ntziachristos V. Drug-based optical agents: infiltrating clinics at lower risk. Sci Transl Med. 2012; 4:134ps11.

113. van Dam, GM. VEGF-targeted Fluorescent Tracer Imaging in Breast Cancer. ClinicalTrialsgov [online]. at <http://www.clinicaltrials.gov/ct2/show/NCT01508572>

114. Gaertner FC, Kessler H, Wester HJ, Schwaiger M, Beer AJ. Radiolabelled RGD peptides for imaging and therapy. Eur J Nucl Med Mol Imaging. 2012; 39:126–138.

115. Muyldermans S, Atarhouch T, Saldanha J, Barbosa JA, Hamers R. Sequence and structure of VH domain from naturally occurring camel heavy chain immunoglobulins lacking light chains. Protein Eng. 1994; 7:1129–1135. [PubMed: 7831284]

116. Oliveira S, et al. Rapid visualization of human tumor xenografts through optical imaging with a near-infrared fluorescent anti-epidermal growth factor receptor nanobody. Mol Imaging. 2012; 11:33–46. [PubMed: 22418026]

117. Bhatia S, Frangioni JV, Hoffman RM, Iafrate AJ, Polyak K. The challenges posed by cancer heterogeneity. Nat Biotechnol. 2012; 30:604–610. [PubMed: 22781679]

118. Gibbs-Strauss SL, et al. Nerve-highlighting fluorescent contrast agents for image-guided surgery. Mol Imaging. 2011; 10:91–101. [PubMed: 21439254]

119. Sheth RA, et al. Improved detection of ovarian cancer metastases by intraoperative quantitative fluorescence protease imaging in a pre-clinical model. Gynecol Oncol. 2009; 112:616–622. [PubMed: 19135233]

120. Mieog JSD, et al. Image-guided tumor resection using real-time near-infrared fluorescence in a syngeneic rat model of primary breast cancer. Breast Cancer Res Treat. 2011; 128:679–689. [PubMed: 20821347]

121. Urano Y, et al. Selective molecular imaging of viable cancer cells with pH-activatable fluorescence probes. Nat Med. 2009; 15:104–109. [PubMed: 19029979]

122. Urano Y, et al. Rapid cancer detection by topically spraying a γ-glutamyltranspeptidase-activated fluorescent probe. Sci Transl Med. 2011; 3:110ra119.

123. Kumar ATNA, et al. Feasibility of in vivo imaging of fluorescent proteins using lifetime contrast. Opt Lett. 2009; 34:2066–2068. [PubMed: 19572001]

124. Themelis G, Yoo JS, Ntziachristos V. Multispectral imaging using multiple-bandpass filters. Opt Lett. 2008; 33:1023–1025. [PubMed: 18451974]

125. Brouwer OR, et al. Image navigation as a means to expand the boundaries of fluorescence-guided surgery. Phys Med Biol. 2012; 57:3123–3136. [PubMed: 22547491]

126. Frangioni JV. Translating in vivo diagnostics into clinical reality. Nat Biotechnol. 2006; 24:909–913. [PubMed: 16900127]

127. Yuasa Y, et al. Sentinel Lymph Node Biopsy Using Intraoperative Indocyanine Green Fluorescence Imaging Navigated with Preoperative CT Lymphography for Superficial Esophageal Cancer. Ann Surg Oncol. 2011; 19:486–493. [PubMed: 21792510]

128. Miyashiro I, et al. Intraoperative Diagnosis Using Sentinel Node Biopsy with Indocyanine Green Dye in Gastric Cancer Surgery: An Institutional Trial by Experienced Surgeons. Ann Surg Oncol. 2012; 20:542–546. [PubMed: 22941164]

129. Miyashiro I, et al. Laparoscopic detection of sentinel node in gastric cancer surgery by indocyanine green fluorescence imaging. Surg Endosc. 2010; 25:1672–1676. [PubMed: 20976497]

130. Kusano M, et al. Sentinel node mapping guided by indocyanine green fluorescence imaging: a new method for sentinel node navigation surgery in gastrointestinal cancer. Dig Surg. 2008; 25:103–108. [PubMed: 18379188]

131. Jeschke S, et al. Visualisation of the lymph node pathway in real time by laparoscopic radioisotope-and fluorescence-guided sentinel lymph node dissection in prostate cancer staging. Urology. 2012; 80:1080–1086. [PubMed: 22990053]

132. Ishizawa T, et al. Indocyanine green-fluorescent imaging of hepatocellular carcinoma during laparoscopic hepatectomy: An initial experience. Asian J Endosc Surg. 2010; 3:42–45.

133. Mitsuhashi N, et al. Usefulness of intraoperative fluorescence imaging to evaluate local anatomy in hepatobiliary surgery. J Hepatobiliary Pancreat Surg. 2008; 15:508–514. [PubMed: 18836805]

134. Hutteman M, et al. Near-infrared fluorescence imaging in patients undergoing pancreaticoduodenectomy. Eur Surg Res. 2011; 47:90–97. [PubMed: 21720166]

135. Tagaya N, et al. Intraoperative exploration of biliary anatomy using fluorescence imaging of indocyanine green in experimental and clinical cholecystectomies. J Hepatobiliary Pancreat Surg. 200910.1007/s00534-009-0195-2

136. Aoki T, et al. Intraoperative fluorescent imaging using indocyanine green for liver mapping and cholangiography. J Hepatobiliary Pancreat Surg. 200910.1007/s00534-009-0197-0

137. Verbeek FPR, et al. Image-guided hepatopancreatobiliary surgery using near-infrared fluorescent light. J Hepatobiliary Pancreat Sci. 2012; 19:626–637. [PubMed: 22790312]

Key points

- NIR fluorescence imaging has been demonstrated to be feasible during cancer surgery using available imaging systems and contrast agents

- Clinical applicability has been described in sentinel lymph node mapping, tumor imaging, visualization of vital structures, and imaging of vascularization and perfusion

- NIR fluorescence image-guided surgery has properties that make it a good candidate for clinical acceptance: fulfills a clinical need, is relatively inexpensive, and fast

- Targeted contrast agents, necessary for full evaluation of this technique, are in advanced stages of clinical approval

- Upcoming years are essential, with novel contrast agents and optimized camera systems the technique should prove its true clinical value
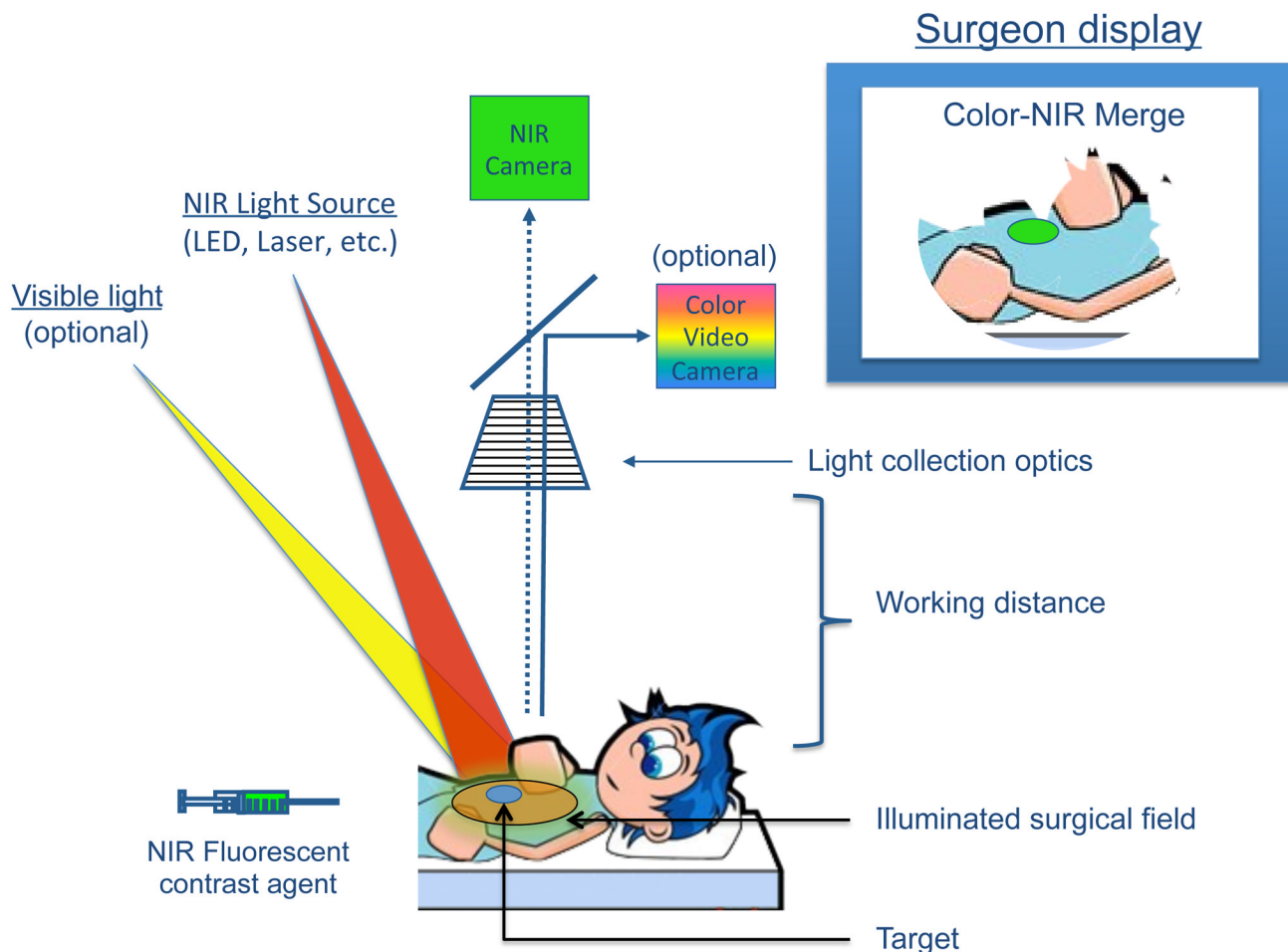
Figure 1. The mechanics of NIR fluorescence imaging
A NIR fluorescent contrast agent is administered intravenously, topically, or intraparenchymally. During surgery, the agent is visualized using a NIR fluorescence imaging system of the desired form factor, i.e., above the surgical field for open surgery or encased within a fiberscope for minimally-invasive and robotic surgery (open surgery form factor shown). All systems must have adequate NIR excitation light, collection optics and filtration, and a camera sensitive to NIR fluorescence emission light. An optimal imaging system includes simultaneous visible (i.e., white) light illumination of the surgical field, which can be merged with NIR fluorescence images. The surgeon display can be one of several forms factors including a standard computer monitor, goggles, or a wall projector (monitor form factor shown). Current imaging systems operate at a sufficient working distance that enables the surgeon to operate and illuminates a sizable surgical field.
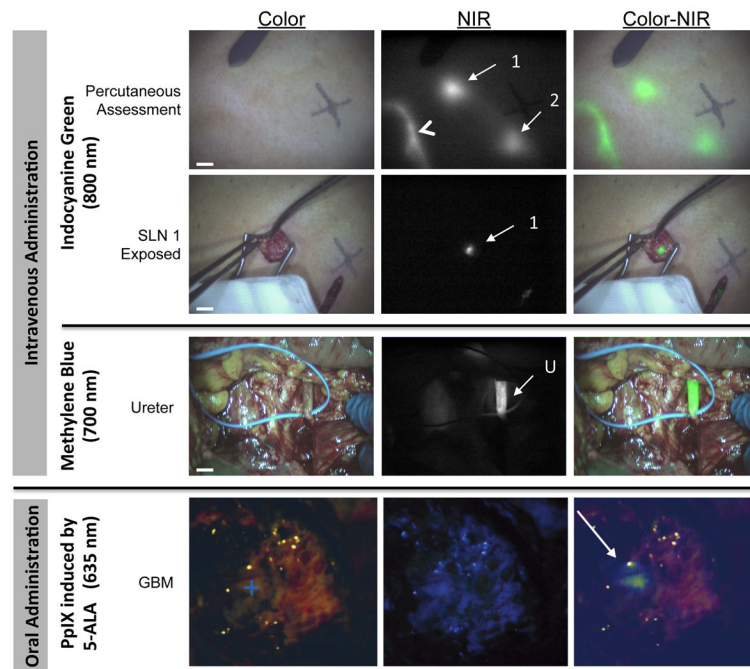
Figure 2. Examples of intraoperative NIR fluorescence imaging

a. Example of SLN mapping using NIR fluorescence imaging in a patient with cutaneous melanoma. Displayed are the color images (left), NIR fluorescence images (middle), and pseudocolored (NIR fluorescence in lime green) merges of the two (right). The lymphatic channel (arrowhead) and SLNs (arrows) can be clearly identified percutaneously and in real-time (top panel). Identification of a SLN (bottom panel) is demonstrated using 800 nm NIR fluorescence imaging 15 min after injection of 1.6 mL of 1000 µM ICG admixed with human serum albumin around the tumor. All images were acquired in real time using the mini-FLARE[12] imaging system. NIR excitation fluence rate was approximately 8 mW/cm^2 and camera exposure time was 10 ms. Scale bars represent 1 cm. Reproduced with permission.[63]

b. Example of NIR fluorescence imaging of the ureter during lower abdominal surgery in a patient with ovarian carcinoma. Intraoperative imaging of the ureter (arrow), 45 min after administration of 1 mg/kg methylene blue. Displayed are the color images (left), 700 nm NIR fluorescence images (middle), and a pseudocolored (NIR fluorescence in lime green) merge of the two (right) acquired with the mini-FLARE imaging system. NIR excitation fluence rate was approximately 1 mW/cm^2 and camera exposure time was 150 ms. Scale bars represent 1 cm. Reproduced with permission.[137]

c. Example of fluorescence imaging in brain surgery during resection of a glioblastoma multiforme (+) using oral 5-ALA-induced PpIX. White light image (left), visible fluorescence (middle) and quantitative fluorescence images overlayed onto white light images (right) are displayed. Reproduced with permission.[39]
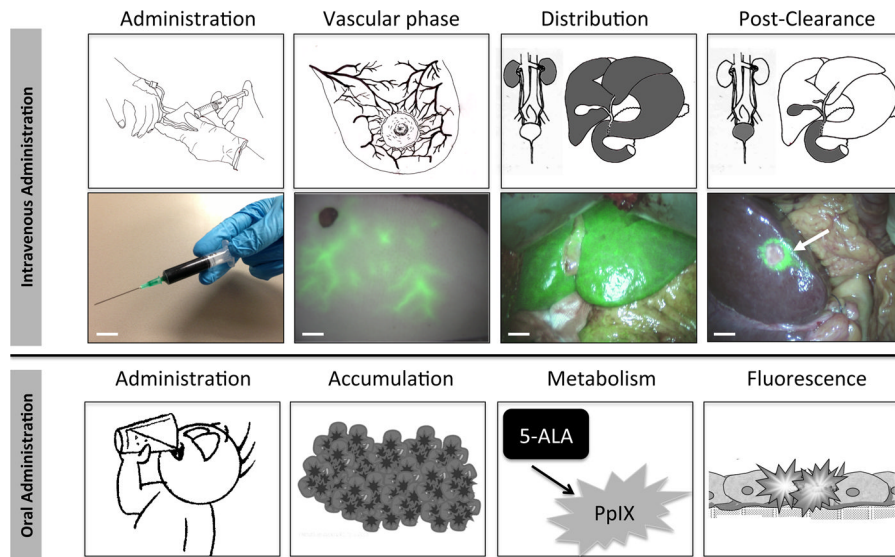
Figure 3. Administration, Biodistribution, and Clearance of a NIR fluorescent contrast agent
Schematic (top row) and clinical example (middle row) of the four key phases of NIR
fluorescence imaging after intravenous administration of a NIR fluorophore. Top-row:
Shown from left-to-right are the different phases over time: first, a NIR fluorescent probe is
administered. After intravenous administration, for example, NIR fluorescence signal is
visualized in the vasculature (second panel). Then, the contrast agent is distributed to all
tissues in the body (third panel) but the target remains obscured. After adequate clearance
time (right panel), adequate contrast between target and surrounding tissue is achieved.
Bottom-row: Left: administration of NIR fluorescent contrast agent. Second panel: ICG
fluorescence as observed in the vasculature of an abdominal tissue flap to be used for breast
reconstructive surgery. Third panel: ICG fluorescence distribution in the liver. Right panel:
ICG clearance from the liver over time, revealing a metastatic colon cancer metastasis
(arrow). Shown in all panels are pseudocolored (lime green) merges of NIR fluorescence
and color video acquired using the mini-FLARE imaging system. Scale bars represent 1 cm.
Bottom row: schematic of the four key phases of NIR fluorescence imaging after
administration of 5-ALA. Shown from left to-right are the different phases over time: first,
the non-fluorescent 5-ALA is orally administered (first panel). After uptake in the
bloodstream via the gastrointestinal tract, the substance accumulates in tumor cells (second
panel), where it is metabolized to the fluorescent protoporphyrin IX (third panel). After
metabolism, tumor demarcation can be visualized using the inherent fluorescent properties
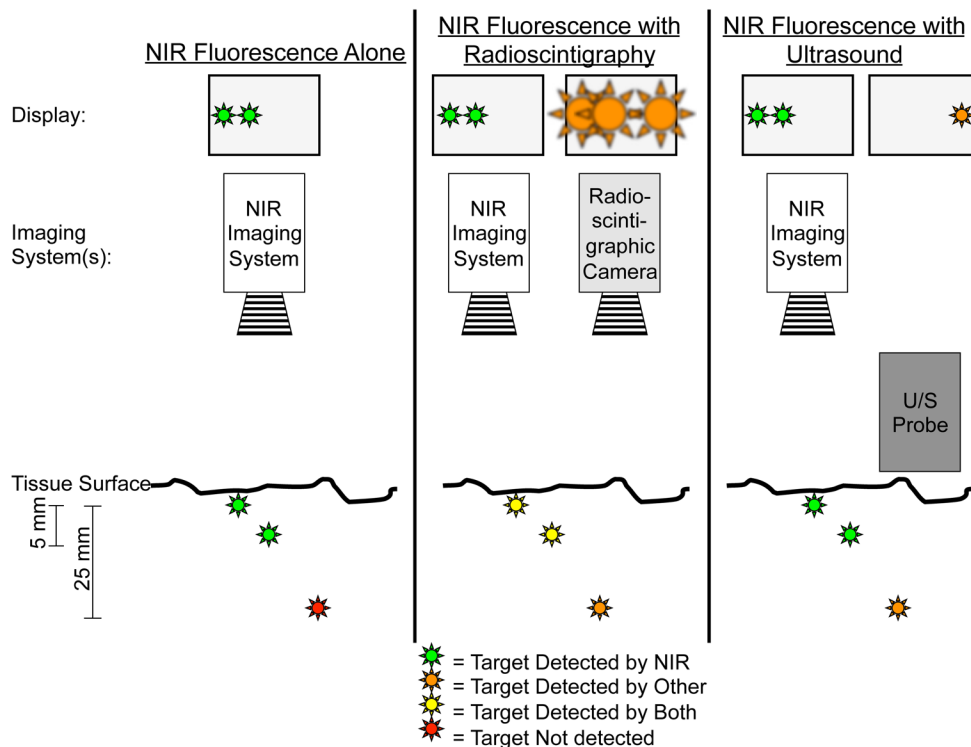of protoporphyrin IX (fourth panel).

Figure 4. NIR fluorescence imaging alone or in combination with other imaging modalities
Left panel: In this example, two superficially located targets, up to 5–8 mm deep, can be located using NIR fluorescence imaging. However, a deeper target at 25 mm would be invisible using by NIR fluorescence imaging alone.
Middle panel: Combining NIR fluorescence imaging with radioscintigraphy enables visualization of all three targets. However, spatial and temporal resolution of radioscintigraphy is poor. Once overlying tissue is removed, as guided by radioscintigraphy, NIR fluorescence can be used for more precise image guidance (see also Figure 2).
Right panel: Intraoperative ultrasound can visualize targets that are located deeper within tissue, but fails to find superficially located targets because of high acoustic reflectance. These superficial targets, though, can be visualized by NIR fluorescence thereby complementing intraoperative ultrasound. Of note, the ultrasound probe must be in direct contact with the tissue being imaged, thus precluding simultaneous imaging with NIR fluorescence.

Table 1

Overview of Clinical Applications

Application	Cancer Type	Imaging System	Contrast Agent	Clinical Status[*]
SLN mapping	Breast	Open	ICG[11,52–56]	Clinical
	Melanoma	Open	ICG[62,63], MMI[69]	Clinical
	Head and Neck	Open	ICG[63,70], MMI[27]	Clinical
	Lung	VATS	ICG[17,71]	Clinical
	Esophagus	Open	ICG[75,127]	Clinical
	Stomach	Open	ICG[74,128]	Clinical
		Lap	ICG[73,129]	Clinical
	Colorectal	Open	ICG[9,130], HSA800 (ex vivo)[59,60]	Clinical
		Lap	ICG[15,58,61]	Clinical
	Cervix	Open	ICG[13,64,65]	Clinical
	Vulvar	Open	ICG[66–68]	Clinical
	Endometrial	Lap	ICG[72]	Clinical
	Prostate	Lap/Rob	ICG[131], MMI[16]	Clinical
	Penile	Open	MMI[69]	Clinical
Tumor imaging (in vivo)	Colorectal liver metastases	Open	ICG[82,83,89]	Clinical
	Hepatocellular carcinoma	Open	ICG[10,82]	Clinical
		Lap	ICG[132]	Preliminary
	Ovarian cancer metastases	Open	ICG[93]	Preliminary
	Breast cancer	Open	Bevacizumab-800CW[113]	Preliminary
	Insulinoma	Open	MB[43]	Preclinical
	Primary solitary tumor of the pancreas	Open	MB[45]	Preliminary
	Bladder cancer	Lap	5-ALA[97]	Clinical
	Brain tumors	Open	5-ALA,[46–48] ICG[91,92]	Clinical
Tumor imaging (topical)	Bladder cancer	Cyst	5-ALA[99], HAL[100]	Clinical
	Colon cancer	Endo	gGlu-HMRG[122]	Preclinical
Vital structures imaging	Bile ducts	Open	ICG[133,134]	Clinical
		Lap	ICG[101,135,136]	Clinical
	Ureters	Open	MB[44]	Preliminary
	Lymph Flow	Open	ICG[55,102]	Clinical
	Nerves	Open	Various[35,118]	Preclinical
Vascularization	Bowel anastomoses	Open	ICG[104,105]	Clinical
		Lap	ICG[106]	Clinical
	Reconstructive surgery	Open	ICG[108–110]	Clinical

[*] Clinical = Multiple independent groups have reported successful application; Preliminary = Initial clinical application has been reported; Preclinical = Application has only been demonstrated in a preclinical setting.

Abbreviations: 5-ALA = 5-aminolevulinic acid; Bevacizumab-800CW = IRDye 800CW conjugated to Bevacizumab; gGlu-HMRG = g-glutamyl hydroxymethyl rhodamine green; ICG = indocyanine green; HAL = hexyl aminolevulinate; HSA800 = IRDye 800CW conjugated to human serum albumin; Lap = laparoscopic surgery; MB = methylene blue; MMI = multimodal imaging agent ICG-^{99m}Technetium-nanocolloid; Rob = robotic surgery; SLN = sentinel lymph node; VATS = video-assisted thoracoscopic surgery;